Pergamon

Acta mater. Vol. 46, No. 7, pp. 2501–2507, 1998

Printed in Great Britain
PII: S1359-6454(97)00409-6
1359-6454/98 $19.00 + 0.00

MODELING OF CHEMICAL WEAR IN FERROUS ALLOYS/ SILICON NITRIDE CONTACTS DURING HIGH SPEED CUTTING

R. F. SILVA[1], F. J. OLIVEIRA[1], F. P. CASTRO[2] and J. M. VIEIRA[1]

Dep. Eng. Cerâmica e do Vidro, Universidade de Aveiro, 3810 Aveiro, Portugal and [2]Dep. Eng. Mecânica, Universidade do Minho, 4810 Guimarães, Portugal

Abstract—The wear resistance of Si_3N_4 in machining of iron alloys can be surprisingly low due to chemical affinity for dissolution in the metal. This limits the use of Si_3N_4 inserts in high speed machining of steels, while Si_3N_4 retains the best performance of all cutting materials in turning of grey cast iron, a different ferrous alloy. The chemical wear of several ceramics has been investigated on the basis of dissolution in pure iron by Kramer and Suh. Nevertheless, the influence of alloy elements was not studied. In the present work, solid solution thermodynamics is applied to predict chemical wear of Si_3N_4 by setting the influence of interaction coefficients of the alloy elements in the Henrian activity of Si and N in austenite. The model predicts the relative order of magnitude of the crater wear of Si_3N_4 inserts in machining of tool steels, carbon steels and grey cast iron. © *1998 Acta Metallurgica Inc.*

1. INTRODUCTION

In the field of cutting tools it is most relevant to study processes of chemical or diffusion wear of Si_3N_4 because of the intimate and strong contact between the ceramic insert and the metal workpiece at high temperatures. Tool degradation results from a combination of mechanical and chemical processes, but in high speed machining of continuous chip forming workpiece materials like the steels, the dominant wear mode is chemical [1, 2]. Even when turning nickel based alloys, Si_3N_4 has only good performance at low speeds showing a quasi-exponential growth of the wear rates with increasing cutting speeds due to diffusion wear [3]. Interdiffusion between elements of the workpiece and tool, solution of tool material and formation of new phases by chemical reactions at the metal/ceramic interface leading to severe crater wear have been reported [1, 4–8]. Interdiffusion weakens the material structure allowing fast disruption of the tool surface [5]. Tonshoff and Bartsch [4] detected components of the ceramic tool material in the secondary flow zone of the metal chip. Depletion of tool elements such as Si and Y at the flank face of the tool confirms that the ceramic dissolves into the hot metal [9].

Thermodynamic calculations addressing the chemical stability of Si_3N_4 and other cutting tool ceramics in machining of iron alloys were performed by Kramer *et al.* [10, 11]. The solubility of the tool was calculated from the free energy of formation of the ceramic material and from the relative partial molar excess free energies of solution of its components in the pure metal. Data clearly showed that wear of oxide tools is not controlled by solubility whereas such wear mode dominates carbide tools. Aronsson [12], in comparative testing of silicon nitride and alumina based cutting tools attributes to chemical inertness the superior crater wear resistance of alumina. However, under conditions of high metal removal rate where toughness and hardness are definitively required, silicon nitride inserts perform better than some alumina tools [13]. Although the thermodynamic approach of Kramer *et al.* has ranked the cutting tool materials in order of the expected reactivity, it has some limitations. It is restricted to the equilibrium with pure iron by not considering the effects of alloying elements. Other authors [1, 7, 14] have explored Kramer's model but some chemical parameters used for the thermodynamic calculations were taken constant over a broad range of temperatures and concentration of alloying elements which is a rather crude approximation. The influence of steel composition in ceramic dissolution was recently investigated by static diffusion couples as a way of predicting chemical wear [7, 15]. The authors used the molecular nitrogen solubility and not the actual Si_3N_4 solubility in steels which can lead to large discrepancies in the final results.

In the present work a model to determine the Si_3N_4 solubility in different iron alloys is developed considering more realistic assumptions for the equilibrium conditions. Experimental values of the solubility products in the solid iron phases and interaction coefficients of all solute atoms were used to calculate the Si and N concentrations in the metal in equilibrium with Si_3N_4. Even conceding that the present thermodynamic model does not take into account reaction kinetics, it gives a realistic measure of the potential for chemical reaction,

the correlation between Si_3N_4 solubility and the crater wear rate of Si_3N_4 based cutting tools being further investigated.

2. THERMODYNAMIC CALCULATIONS OF Si_3N_4 SOLUBILITY IN IRON ALLOYS

Iron alloys are multicomponent solid solutions in Fe where alloying elements strongly interact with one another. The solubility of Si_3N_4 in distinct iron alloys will be calculated at a reference temperature of 1000°C, which is representative of the conditions developed at the contact between the metal chip and the rake face of the ceramic tool during high speed cutting. Fe and Si_3N_4 react at 950°C and above [16]. Equilibrium within the γ-Fe phase is considered for thermodynamic evaluation of Si_3N_4 solubility in solid iron. Cast iron, carbon and chromium alloyed steels represent broad classes of iron alloys that have been investigated in relation to the benefits of high speed machining with ceramic cutting inserts [1–9]. In the analysis of crossed chemical interactions, Cr–N interaction competes with the dissolution of Si_3N_4 and molecular N_2 in austenitic iron. The chemical equilibria for phase compatibility in the Si_3N_4–CrN–$(\gamma\text{-Fe})_{ss}$ system are given in Table 1. By convenience, the activities of the alloying elements and Si and N from the Si_3N_4 ceramic tool in iron, will be defined on a weight percent basis using Henry's law for dilute systems [17]:

$$\log(h_i) = \log[\%i] + \sum_j e_i^j [\%j] \qquad (1)$$

where h_i is the Henrian activity of the i element, $[\%i]$ and $[\%j]$ are the concentrations in weight percent of the i and j elements dissolved in the alloy. The changes of chemical activity of those elements in the γ-Fe solid solution is expressed by the first order interaction coefficients e_j^i. Information on e_j^i values, namely in γ-Fe, is scarce compared to data for liquid iron. However, as described below, values of coefficients e_j^i were calculated from analysis of published phase diagrams or were estimated from numerical data available for liquid iron and for α-Fe. In some cases transposed e_i^j values were assessed from the corresponding published values of e_j^i parameters in γ-Fe, by applying a procedure given by Lupis [18]:

$$e_i^j = \frac{M_i}{M_j} e_j^i + \frac{1}{230} \frac{M_j - M_i}{M_j} \qquad (2)$$

where M is the atomic weight of the element. The complete set of interaction coefficients needed for the calculation of solubility in the different iron alloys was calculated as described in the following.

Table 1. Chemical equilibria in Si_3N_4/Fe-alloys interactions

Chemical equilibrium	Equilibrium constant	Equation
$Si_3N_4 = 3Si^a + 4N$	K_I	(3)
$Cr + N = CrN$	K_{II}	(4)
$Si_3N_4 + 4Cr = 3Si + 4CrN$	K_{III}	(5)
$1/2N_2 = N$	K_{IV}	(6)

[a]The dissolved species in austenitic iron appear italic.

Table 2. Dependence of first order interaction coefficients on temperature

$e_i^j(T) = a + b/T$			
e_i^j	a	b	Ref.
e_{Si}^{Si}	−0.135	364	[16, 19]
e_N^{Si}	−0.110	274	[16]
e_N^N	—	109	[16]
e_C^{Si}	—	128	[16]

2.1. *First order interaction coefficients e_i^j in γ-iron*

A summary of known values of first order interaction coefficients as a function of temperature is given in Table 2. e_{Si}^{Si} for γ-Fe was considered the same as that for α-Fe [16] due to the narrow two-phase transition between the γ-loop and α region in the Fe–Si phase diagram [19]. e_N^{Si}, e_N^N and e_C^{Si} were derived by Kunze *et al.* [16]. The Raoultian interaction coefficient in γ-Fe, $\varepsilon_{Si}^{Cr} = 0.05$ [20] was converted to the Henrian interaction coefficients, giving $e_{Si}^{Cr} \approx 0$ and $e_{Cr}^{Si} \approx 0$. $e_{Cr}^{C} = -0.051$ and $e_C^C = 0.18$ were estimated from the Raoultian interaction coefficients at 1273 K, $\varepsilon_C^{Cr} = -10.9$ [18] and $\varepsilon_C^C = 8.7$ [18], respectively. No value of e_{Cr}^{Cr} in γ-Fe was found in the literature, but self interaction coefficients are usually very small as it is the case of e_{Cr}^{Cr} in liquid iron (−0.0003) [21]. So this value is approached to zero.

Kagawa *et al.* [22] measured the solubility of nitrogen in austenite in equilibrium with gaseous N_2 at 1 atm, in a Fe–C–N alloy, equation (6) in Table 2. By applying equation (1) the expression of the equilibrium constant K_{IV} for equation (6) can be rearranged to:

$$\log[\%N] + 0.086[\%N] = \log K_{IV} - e_N^C[\%C] \qquad (7)$$

e_N^N being given in Table 3. The first term of this equation is plotted against [%C] in Fig. 1 taking the values of [%N] and [%C] at the solubility limit in austenite [22]. Linear regression analysis gives $e_N^C = 0.075$, the transpose e_C^N given by equation (2).

The interaction coefficients for the different alloys studied in the present paper are summarized in Table 3 for the temperature of 1273 K. Equation (2) was applied to calculate e_{Si}^N, e_{Si}^C as the transpose of e_N^{Si} and e_C^{Si}, respectively. The value of e_{Cr}^N is calcu-

Table 3. First order interaction coefficients e_i^j in γ-Fe at 1273 K

i	j			
	Si	N	C	Cr
Si	0.15	0.21	0.23	0
N	0.11	0.086	0.075	−0.10
C	0.10	0.065	0.18	−0.051
Cr	0	−0.40	−0.24	0

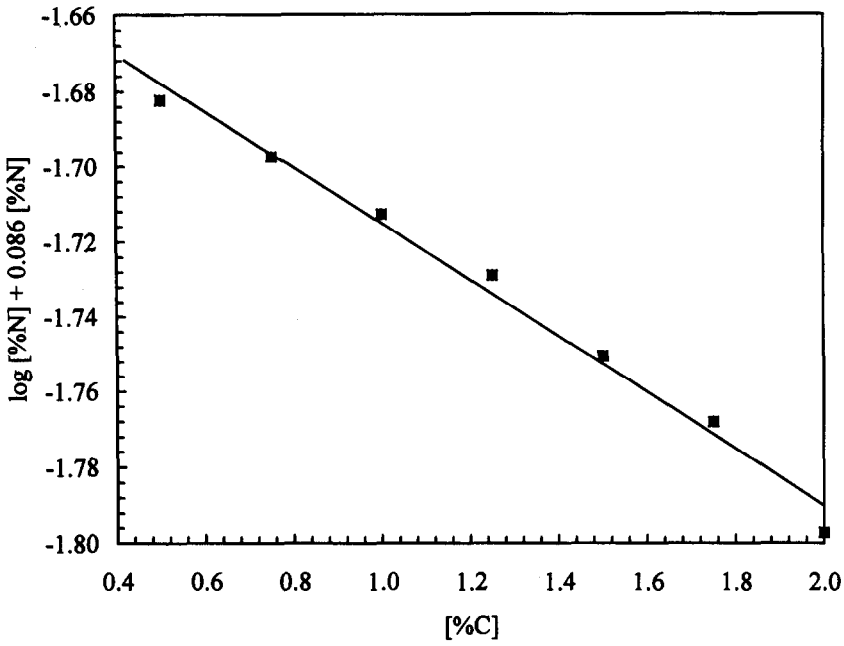

Fig. 1. Graphical determination of e_N^C by equation (7).

lated in the section on chromium alloyed steels, below.

2.2. *Dissolution of Si_3N_4 in pure iron*

The concentration of Si and N in pure γ-iron at 1000°C in equilibrium with silicon nitride is calculated from data of the work of Kunze *et al.* [16]. The equations for nitrogen concentration in austenitic and ferritic iron and the solubility product of Si_3N_4 in ferritic iron are summarized in Table 4. Equations (8)–(10) can be rearranged to the form of equation (11):

$$3\log[\%Si] + 4\log[\%N] = -\frac{15541.6}{T} - 37.432 + 14.732\log T - \frac{436}{T}[\%N] \quad (11)$$

Si concentration in γ-Fe was considered equal to the concentration in α solid solution for the reason presented above that the effect of Si solubility on the thermodynamic properties of both crystalline structures is virtually the same [19]. At 1273 K, equation (11) becomes:

$$\log[\%Si] = -1.300 - 1.333\log[\%N] - 0.114[\%N] \quad (12)$$

By assuming Henry's law, equation (1), the equation of the solubility constant K_I for Si_3N_4 dissolution in γ-Fe, equation (3) in Table 2 expands to:

$$\log K_I = 3\log[\%Si] + 4\log[\%N] + 3(e_{Si}^{Si}[\%Si] + e_{Si}^{N}[\%N]) + 4(e_N^N[\%N] + e_N^{Si}[\%Si]) \quad (13)$$

Rearranging equation (13) with equation (11) and e_{Si}^{Si}, e_N^{Si}, e_N^N and e_{Si}^N in Table 3 gives:

$$\log K_I = -\frac{15541.6}{T} - 37.432 + 14.732\log T + \left(\frac{2188}{T} - 0.845\right)[\%Si] + \left(\frac{1644}{T} - 0.672\right)[\%N] \quad (14)$$

which is the equation for the solubility constant of silicon nitride dissolution in pure γ-Fe. The range

Table 4. Temperature dependence of the Si and N concentration in ferritic and austenitic iron [16]

Chemical equilibrium	Equation
$\log[\%N]_\alpha = -\frac{1606}{T} - 3.511 + \frac{1}{2}\log P_{N_2}$	(8)
$\log[\%N] = \frac{2833.6}{T} - 17.719 + 3.683\log T - \frac{109}{T}[\%N] + \frac{1}{2}\log P_{N_2}$	(9)
$\log([\%Si]_\alpha^3[\%N]_\alpha^4) = -\frac{33300}{T} + 19.4$	(10)

Note: $[\%i]_\alpha$ and $[\%i]$ are the concentrations by weight percent of i element in ferrite and austenite, respectively.

of solubility measurements used to derive equations (8)–(10) was $0.48 < [\%Si] < 0.75$ [16]. For the mean silicon concentration of [%Si] = 0.61% and the resulting value of [%N] = 0.15 by equation (12), equation (14) gives $\log K_I = -3.27$ at 1273 K.

2.3. Si_3N_4 dissolution in chromium alloyed steels

The interaction of chromium with nitrogen from the Si_3N_4 ceramic tool is very strong for a chromium alloyed steel and CrN precipitates in γ-Fe phase for concentrations well below 13 wt%Cr at 1273 K [23]. Equation (4) in Table 1 must be added to the solubility [equation (3)] of the ceramic, leading to global equation (5).

The equilibrium constant K_{II} depends on the Cr and N concentrations in γ-Fe and on the interaction coefficients, equation (1) as follows:

$$\log K_{II} = -\log[\%Cr] - \log[\%N] - (e_{Cr}^{Cr}[\%Cr] + e_{Cr}^{N}[\%N]) - (e_{N}^{N}[\%N] + e_{N}^{Cr}[\%Cr]) \quad (15)$$

Using equation (2) to express e_N^{Cr} as a function of e_{Cr}^N and replacing e_{Cr}^{Cr} and e_N^N by their respective values at 1273 K, Table 3, equation (15) is rearranged to:

$$\log[\%Cr] + \log[\%N] + 0.086[\%N] - 0.0032[\%Cr] = -\log K_{II} - ([\%N] + 0.2692[\%Cr])e_{Cr}^{N} \quad (16)$$

The values of $\log K_{II}$ and e_{Cr}^N are obtained by lineal regression analysis from the [%Cr] and [%N] values at the solubility limit line of CrN in γ-Fe field of the Fe–Cr–N phase diagram at 1273 K [23]. The first member of equation (16) is plotted against ([%N] + 0.2692 [%Cr]) as shown in Fig. 2, giving the values of $K_{II} = 0.86$ and $e_{Cr}^N = -0.40$.

From the chemical equilibria I, II and III in Table 1, and the above values of K_I and K_{II} at 1273 K,

$$\log K_{III} = \log K_I + 4 \log K_{II} = 0.17 \quad (17)$$

On the other hand, $\log K_{III}$ can be written as:

$$\log K_{III} = 3\log[\%Si] - 4\log[\%Cr] + 3(e_{Si}^{Si}[\%Si] + e_{Si}^{N}[\%N] + e_{Si}^{C}[\%C] + e_{Si}^{Cr}[\%Cr]) - 4(e_{Cr}^{Cr}[\%Cr] + e_{Cr}^{N}[\%N] + e_{Cr}^{C}[\%C] + e_{Cr}^{Si}[\%Si]) \quad (18)$$

Replacing all the known parameters in equation (18), the general equation for Si and N solubilities in the γ phase of chromium alloyed steels thus becomes:

$$[\%N] = 0.076 - 1.35\log[\%Si] - 0.20[\%Si] + 1.79\log[\%Cr] - 0.74[\%C] \quad (19)$$

The carbon and chromium content in the first chromium alloyed steel in Table 5, the DIN 1.2080 tool steel, are above the solubility limit in γ-Fe at 1273 K, while these same alloying elements are fully dissolved in the DIN 1.4021 steel at the reference temperature [24]. The saturation contents of carbon and chromium in γ-Fe at 1273 K for the 2.0 wt%C,

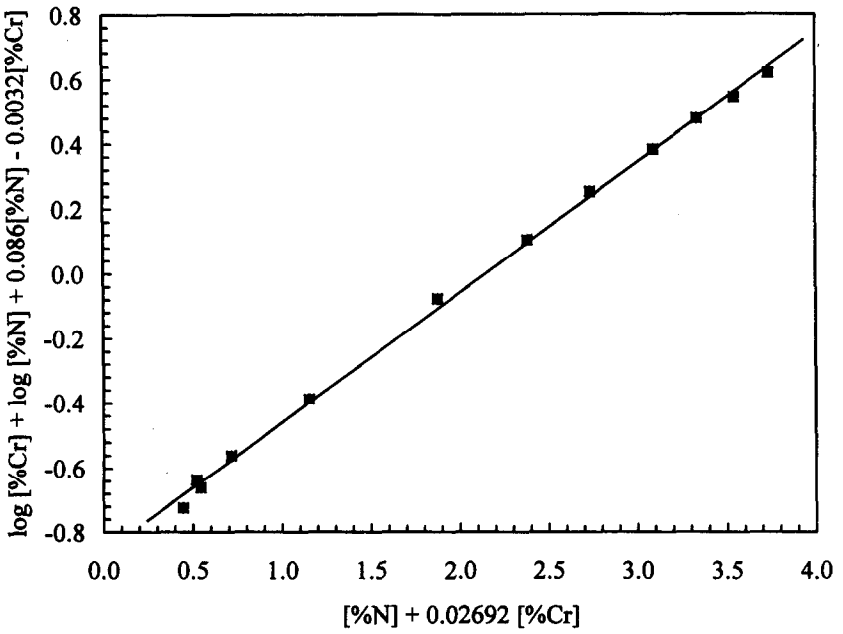

Fig. 2. Graphical determination of e_{Cr}^N and solubility constant K_{II} by equation (16).

Table 5. Si, N and Si_3N_4 equilibrium solubilities in the metal chip and crater wear parameter κ

Metal	Si (wt%)	N (wt%)	Si_3N_4 (cm^3/mol Fe)	Relative Si_3N_4 solubility	κ
Pure iron	0.34	0.23	0.10	26	—
2 wt%C, 12 wt%Cr steel (DIN 1.2080)	0.80	0.53	0.23	59	9.4×10^{-6} [a], 2.6×10^{-6} [b]
0.2 wt%C, 13 wt%Cr steel (DIN 1.4021)	1.82	1.21	0.53	136	—
3.9 wt%C, 2.9 wt%Si gray cast iron	0.014	0.009	0.0039	1	1.1×10^{-7} [a]
0.42 wt%C carbon steel (DIN 1.1186)	0.32	0.21	0.093	24	1.6×10^{-6} [c], 8.2×10^{-7} [c]

[a] Si_3N_4 CeO_2 ceramic tool [5].
[b] Si_3N_4–AlN–CeO_2 ceramic tool [5].
[c] Commercial silicon nitride inserts [6].

12 wt%Cr steel were determined from the isothermal section of the Fe–Cr–C phase diagram at 1273 K [24]. For the approximate saturation values of [%C] = 0.9 and [%Cr] = 4.4 the final relationship between the concentrations of Si and N in γ-Fe for the DIN 1.2080 tool steel becomes:

$$[\%N] = 0.56 - 1.35 \log[\%Si] - 0.20[\%Si] \quad (20)$$

For a 0.2 wt%C, 13 wt%Cr steel, the isothermal section of the Fe–Cr–C phase diagram at 1273 K shows that all the carbon and chromium are dissolved in γ-Fe [24]. By straightforward replacing the nominal [%C] and [%Cr] values of the alloy in equation (19), yields:

$$[\%N] = 1.92 - 1.35 \log[\%Si] - 0.20[\%Si] \quad (21)$$

2.4. Si_3N_4 dissolution in grey cast iron and carbon steels

The solubility constant, K_1, for the dissolution of silicon nitride in γ-Fe phase of grey cast iron and carbon steels can be expressed by equation (13) with addition of the first order interaction coefficients of carbon on silicon and nitrogen, in due proportions. Replacing K_1 for its value at 1273 K ($K_1 = -3.27$), e_{Si}^{C} and e_{N}^{C} for the values given in Table 3, the final equation is obtained:

$$\log[\%Si] + 0.3[\%Si] = -1.09 - 1.333 \log[\%N] - 0.325[\%N] - 0.33[\%C] \quad (22)$$

As before, grey cast iron represents an alloy where the alloying elements exceed the solubility limit in γ-Fe, while they are fully dissolved in carbon steels. The saturation solubilities for carbon and silicon in γ-Fe at 1273 K were graphically determined from an isothermal section of the Fe–Si–C phase diagram at 1273 K [24]. The approximate value of [%C] = 1.0 was found for the nominal Si content of the grey cast iron composition in Table 5 ([%Si] = 2.9). The remaining carbon precipitates as graphite. The elements Mn and S of the cast iron composition precipitate as MnS and should not interfere with the equilibria set in Table 1. By replacing these values of [%C] and [%Si] in equation (22), the calculated value of the solubility of N in γ-Fe phase of grey cast iron becomes [%N] = 0.009.

The silicon and nitrogen solubilities in carbon steels can be calculated by replacing the carbon content [%C] in equation (22). For a 0.42 wt%C carbon steel, Table 5, this relationship is thus:

$$\log[\%Si] + 0.3[\%Si] = -1.229 - 1.333 \log[\%N] - 0.325[\%N] \quad (23)$$

3. DISCUSSION

The results of the precedent section can lead to the estimation of the chemical wear of silicon nitride in contact with ferrous alloys. The Si and N saturation in the metal chip is given by equations (12), (20), (21) and (23) for pure iron and for chromium alloyed and carbon steels, respectively. The relationship between Si and N equilibrium concentration for each alloy is plotted in Fig. 3, together with the point representative of the nitrogen solubility in the gray cast iron as calculated in Section 2.4. The concentrations of Si and N in iron in equilibrium with the Si and N source, the Si_3N_4 ceramic, is given by the interception points of the saturation curves with the straight line representing the stoichiometric Si_3N_4 composition. The resulting solubility values span into a range of two orders of magnitude showing that the composition of the ferrous alloy strongly affects the wear resistance of the silicon nitride cutting tools.

Table 5 gives the equilibrium solubilities of Si, N and the concentration of dissolved Si_3N_4 in equilibrium with the selected alloys at 1273 K as well as the values of the crater wear parameter κ obtained in a previous work for DIN 1.2080 tool steel and gray cast machining [5] and from literature, for 0.42 wt%C carbon steel turning [6]. κ is defined as $\kappa = \Gamma/M$, the ratio between the crater wear rate, (Γ = KM·KT/t; KM being the distance between the tool edge and crater center, KT the crater depth and t the cutting time) and the metal removal rate (M = cutting speed × feed) [5]. The Si_3N_4 solubility is normalized to the lowest value, the value in the gray cast iron in Table 5. It becomes evident that additions of C or Si to the Fe alloy decrease Si_3N_4

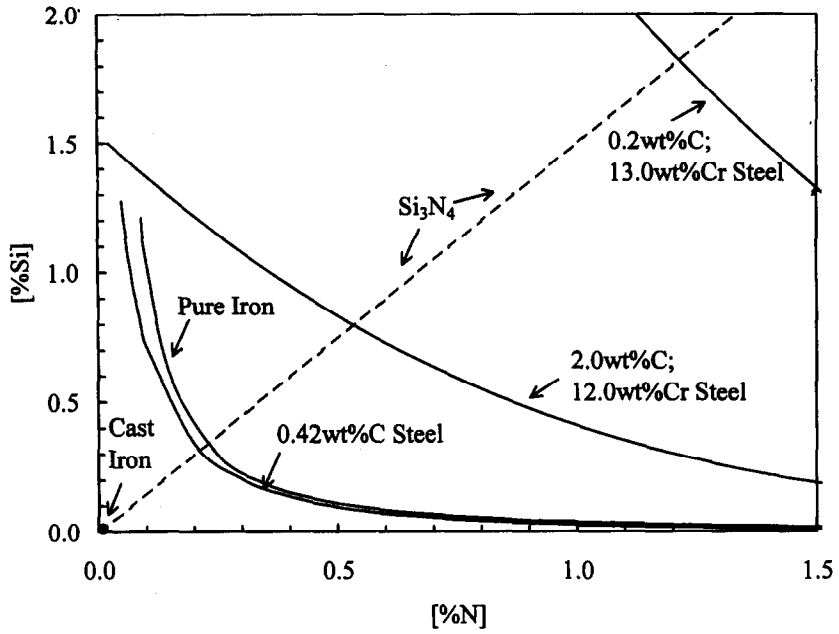

Fig. 3. Equilibrium solubility lines of Si and N in γ-Fe at 1273 K for distinct iron alloys.

solubility, the alloying with Cr having the opposite effect. These results corroborate the observations that silicon nitride tools present the highest resistance to wear by dissolution when machining gray cast iron [1, 4, 5, 13] as given by the low value of κ. In Fig. 4 the wear parameter κ is plotted against Si_3N_4 solubility in a log–log scale, resulting in a straight line of slope unity, the two variables being directly proportional. The scatter of crater wear parameter κ for each type of alloy in Fig. 4 are mostly due to differences of secondary phases used as sintering aids of the silicon nitride insert materials [5], Table 5. It is thus possible to predict relative wear rates of Si_3N_4 cutting tools when machining different ferrous alloys using the chemical wear model.

Although other models [1, 7, 10, 11, 14, 15] were developed to predict relative wear rates of ceramic cutting tools based on thermodynamics, there are some important differences with respect to the pre-

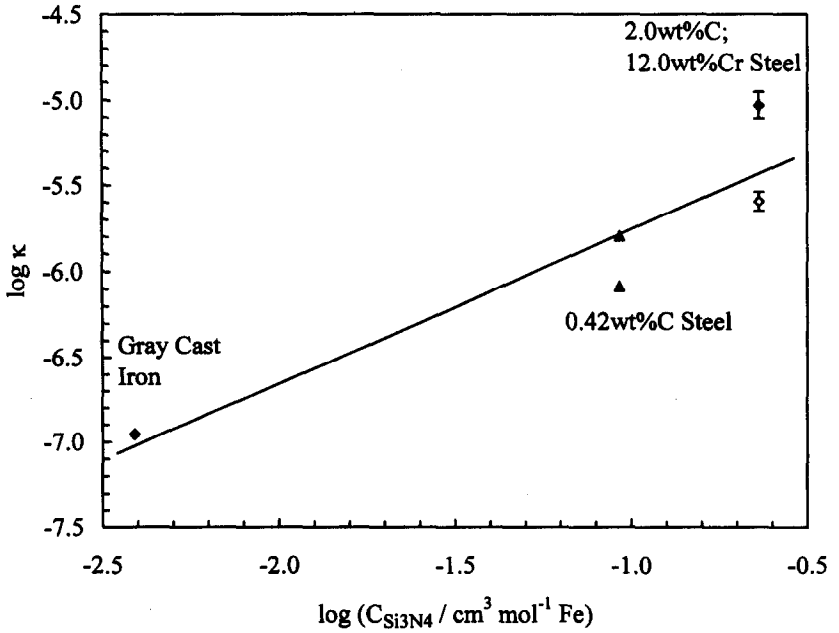

Fig. 4. Relationship between crater wear parameter κ and Si_3N_4 solubility in γ-Fe. (●, ■) Si_3N_4–CeO_2 ceramic tool [5]; (○) Si_3N_4–AlN–CeO_2 ceramic tool [5]; (▲) commercial silicon nitride inserts [6].

sent model that are highlighted. The early studies of Kramer *et al.* [10, 11] have only considered tool wear by solution in pure α-Fe and postulated that the α-Fe is preserved in the metastable form at the high temperatures developed during cutting. Since seizure conditions occur at the contact between the chip and the tool rake face [5, 25], the equilibrium structure, γ-Fe, is used in the present study for the calculation of solubilities. It should be pointed out that the results of static ceramic/metal interaction diffusion couples are often performed above 1273 K, where no doubts exist about the α/γ-Fe transformation. The reactivity of the diffusion couples was tentatively correlated to chemical wear in turning by using Kramer's model [1, 7].

The Si_3N_4 solubility in pure iron calculated by the model of Kramer has a value of 0.74 cm^3/mol Fe [10] which is much higher than the value in Table 5. The discrepancy cannot be attributed to differences of the iron crystalline structures adopted in the two models because a calculation made with the solubility constant as experimentally determined in α-Fe, yields a value of 0.04 cm^3/mol Fe [16]. In the model of Kramer the relative partial molar excess free energies of Si and N were estimated at 1600 K, for a Fe–19 at%Si alloy in equilibrium with liquid iron and N_2 gas saturated iron, respectively. These values were later used irrespectively of the actual values of Si and N concentrations and of temperature [7]. Furthermore, self interaction coefficients are only implicit in those procedures, such approximations giving rise to large uncertainties in any final quantitative result. Vleugels *et al.* introduced interaction coefficients to distinguish the chemical reactivity of sialon ceramics with several iron alloys [7, 14, 15]. The thickness of the reacted layer in metal/sialon static couples correlates in a non straightforward way to the calculated nitrogen solubilities [15]. However these values of nitrogen solubility have not considered Si solution from Si_3N_4 and its effect on N solubility, a level of correction that can only be achieved if all of the most intensive crossed interactions are taken into account as in Table 3.

4. CONCLUSIONS

The values of the first order interaction coefficients of N, Si and alloying elements in γ-Fe were reviewed. It is shown that the first order interaction coefficients of dissolving and alloying elements on N, Si, C and Cr in the austenitic phase bear additional contributions to the Si_3N_4 solubility in the iron alloys which happen to be as strong as those of the elements on the N alone.

The results of the present thermodynamic model were able to predict relative wear rates of silicon nitride base inserts in the machining of iron alloys. This thermodynamic tool also allows the calculation of Si_3N_4 solubility lines in iron alloys phase diagrams. The concept can be adopted to alloying elements other than Si, N, C and Cr. This method is restricted so far to Si_3N_4 but it can be extended to sialons, composites or even to other ceramic materials giving a more consistent approach than those reported.

Acknowledgements—The financial support from JNICT under the research contract PBIC/C/CTM/1917/95 is gratefully acknowledged. F. J. O. acknowledges the financial support of the Sub-Programa Ciência e Tecnologia do 2º Quadro Comunitário de Apoio.

REFERENCES

1. Buljan, S. T. and Wayne, S. F., *Wear*, 1989, **133**, 309.
2. Buljan, S. T. and Wayne, S. F., *Adv. Ceram. Mater.*, 1987, **2**, 813.
3. Baldoni, J. G. and Buljan, S. T., *Ceram. Bull.*, 1988, **67**, 381.
4. Tönshoff, H. K. and Bartsch, S., *Can. Metall. Q.*, 1989, **28**, 353.
5. Silva, R. F., Gomes, J. M., Miranda, A. S. and Vieira, J. M., *Wear*, 1991, **148**, 69.
6. Yeomans, J. A., Ph.D. Thesis, University of Cambridge, Cambridge, 1986.
7. Vleugels, J., Jacobs, P., Kruth, J. P., Vanherck, P., Du Mong, W. and Van Der Biest, O., *Wear*, 1995, **189**, 32.
8. Lo Casto, S., Lo Valvo, E., Ruisi, V. F., Lucchini, E. and Maschio, S., *Wear*, 1993, **160**, 227.
9. Kannatey-Asibu, E., *J. Manufact. Syst.*, 1990, **9**, 159.
10. Kramer, B. M. and Suh, N. P., *J. Eng. Ind.*, 1980, **102**, 303.
11. Kramer, B. M. and Judd, P. K., *J. Vac. Sci. Technol. A*, 1985, **3**, 2439.
12. Aronsson, B., *Powder Metall. and Related High Temperature Materials*, Bombay, India, 14–17 December 1983, p. 319.
13. Blackman, T. N., *The Foundryman*, January 1990, p. 17.
14. Vleugels, J. and Van Der Biest, O., *Third Euro-Ceramics*, Vol. 1, ed. P. Duran and J. F. Fernandez, Faenza Editrice Ibérica S. L., Spain, 1993, p. 1121.
15. Vleugels, J., Vandeperre, L. and Van Der Biest, O., *J. Mater. Res.*, 1996, **11**, 1265.
16. Kunze, J., Pungun, O. and Friedrich, K., *J. Mater. Sci. Lett.*, 1986, **5**, 815.
17. Parker, R. H., *An Introduction to Chemical Metallurgy*. Pergamon Press, Oxford, 1978.
18. Lupis, C. H. P., *Chemical Thermodynamics of Materials*. North-Holland, New York, 1983.
19. Hansen, M., *Constitution of Binary Alloys*, 2nd Edn. McGraw-Hill, New York, 1958.
20. Fujisawa, T., Kimura, S. and Sakao, H., *Tetsu To Hagane*, 1981, **67**, 940.
21. Sigworth, G. K. and Elliot, J. F., *Metal Sci.*, 1974, **8**, 298.
22. Kagawa, A., Okamoto, T. and Goda, S., *J. Mater. Sci.*, 1988, **23**, 649.
23. Hertzman, S. and Jarl, M., *Metall. Trans. A*, 1987, **18A**, 1745.
24. *Metals Handbook* Vol. 3, American Society for Metals, Metals Park, OH, 1992.
25. Trent, E. M., *Metal Cutting*. Butterworths, Guildford, 1984.